New Perspectives in Spintronic and Mesoscopic Physics (NPSMP2015)
Kashiwa, Jun. 12, 2015

Helical transport in helical crystals

Shuichi Murakami
Department of Physics, Tokyo Tech.
TIES, Tokyo Tech.

Inversion asymmetric systems i.e. Te (tellurium)

- Weyl semimetals
- Chiral transport in crystals with helical lattice structure

Hirayama, Okugawa, Ishibashi, SM, Miyake, PRL 114, 206401 (2015)

Collaborators:

- Tokyo Tech.
  M. Hirayama, T. Yoda, T. Yokoyama, M. Noro
- AIST, Tsukuba, Japan
  T. Miyake, S. Ishibashi

NI-TI phase transitions and Weyl semimetals

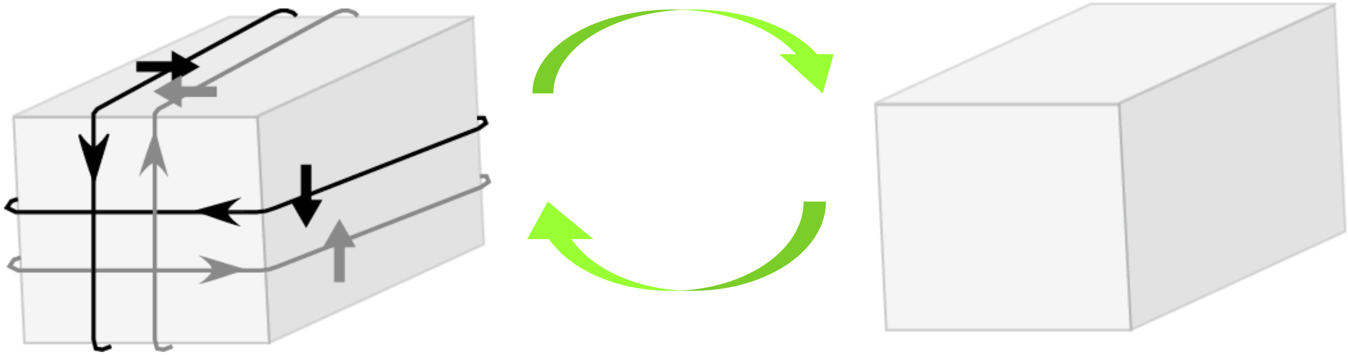

TI: topological insulator

NI: normal insulator

SM, New J. Phys. ('07).
SM. Kuga, PRB ('08)
SM, Physica E43, 748 ('11)

Z_2 topological number ν

ν=0: normal insulator (NI)
ν=1: topological insulator (TI)

(A) systems without inversion symmetry	(B) systems with inversion symmetry
$$(-1)^{\nu} = \prod_i \frac{\sqrt{\det[w(\Gamma_i)]}}{\mathrm{Pf}[w(\Gamma_i)]}$$ $w_{mn}(\vec{k}) = \langle u_{-k,m} \vert \Theta \vert u_{k,n} \rangle$ Γ_i : TRIM Fu,Kane, PRB(2006)	$$(-1)^{\nu} = \prod_i \prod_{m=1}^{N} \xi_{2m}(\Gamma_i)$$ Parity eigenvalue $\begin{cases} +1: \text{symmetric} \\ -1: \text{asymmetric} \end{cases}$ Fu,Kane, PRB(2007)

Formulae are different between (A) & (B)

→ How does the TI-NI phase transition occur in (A) & (B)?

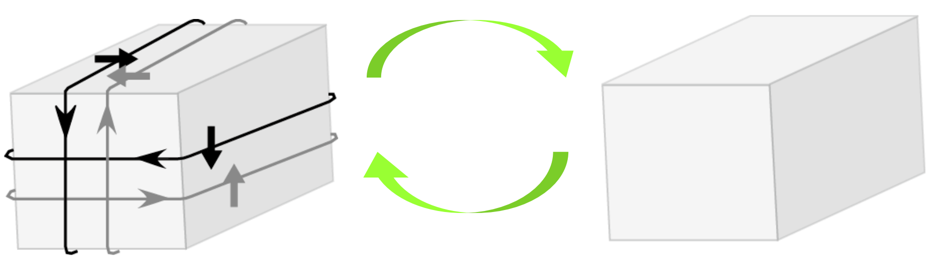

Universal phase diagram in 3D

SM, New J. Phys. ('07).
SM. Kuga, PRB ('08)
SM, Physica E43, 748 ('11)

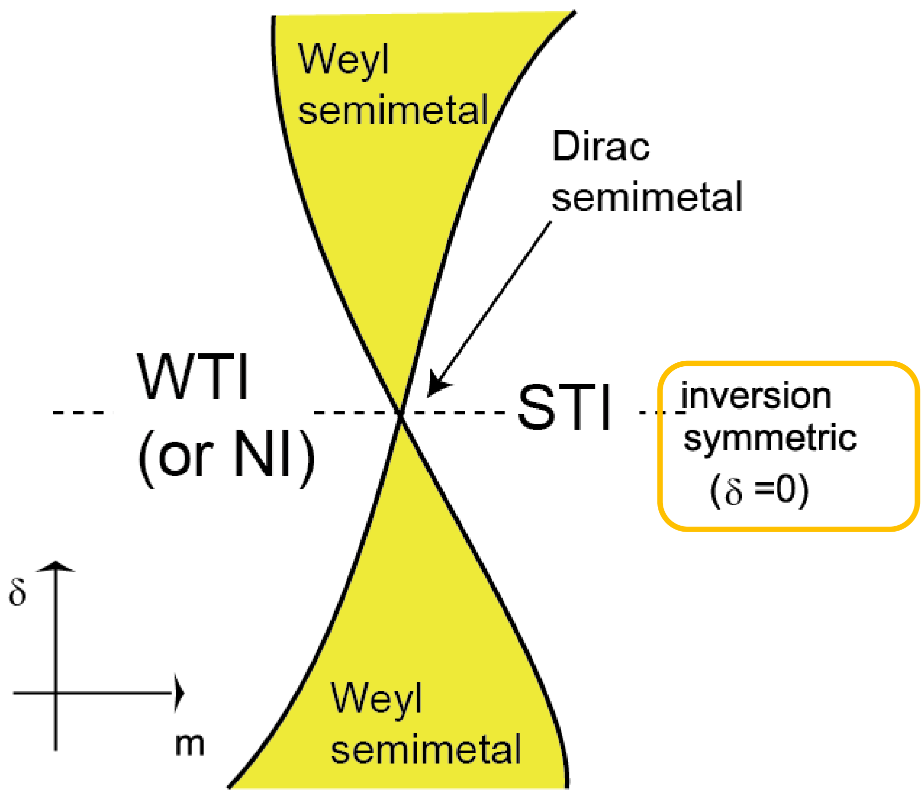

(δ : inversion symmetry breaking)
(m : external parameter)

Systems with inversion symmetry

- Gap closes at TRIM
  inversions between two bands with opposite parities.
- Insulator-to-insulator transition

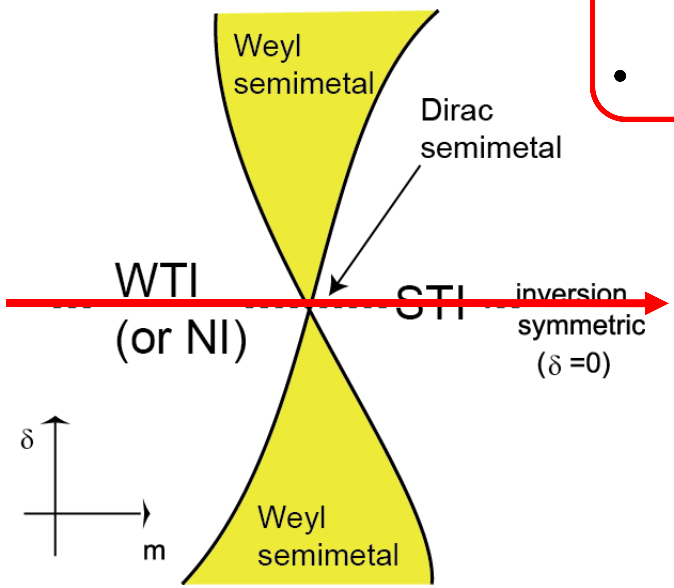

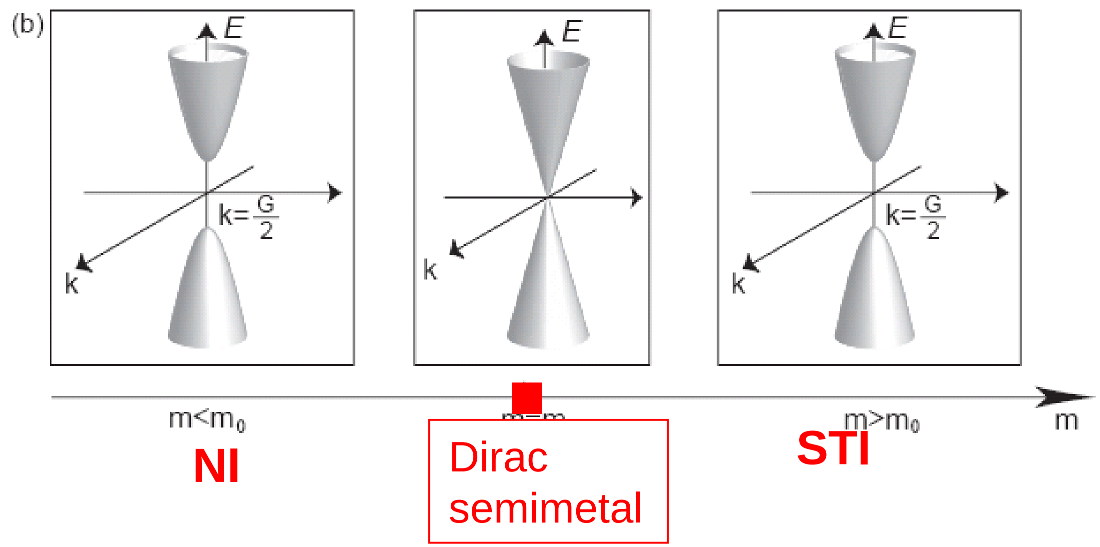

e.g. $TlBi(S_{1-x}Se_x)2$

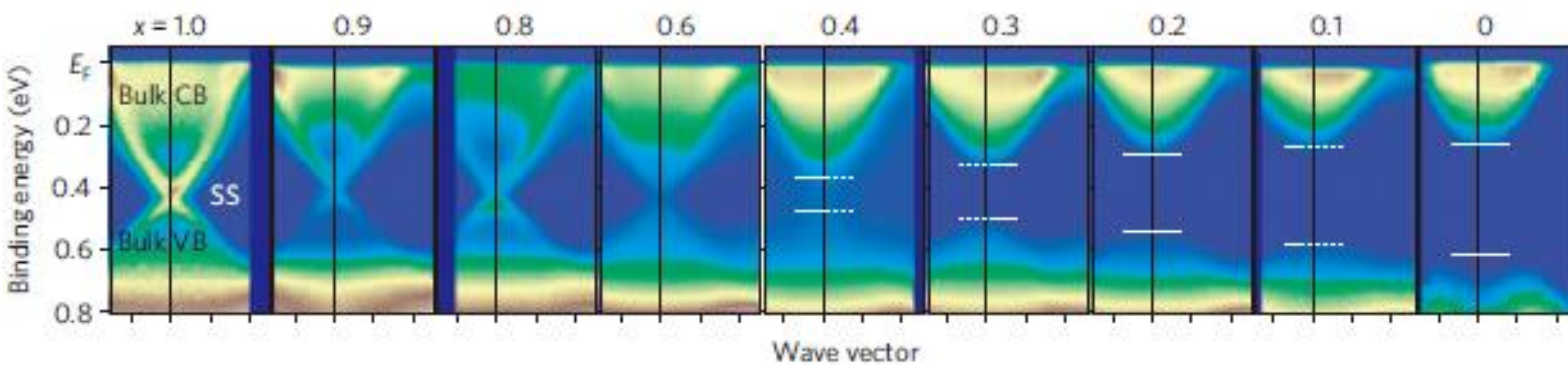

Sato et al., Nature Phys.7, 840 ('11)

Systems without inversion symmetry

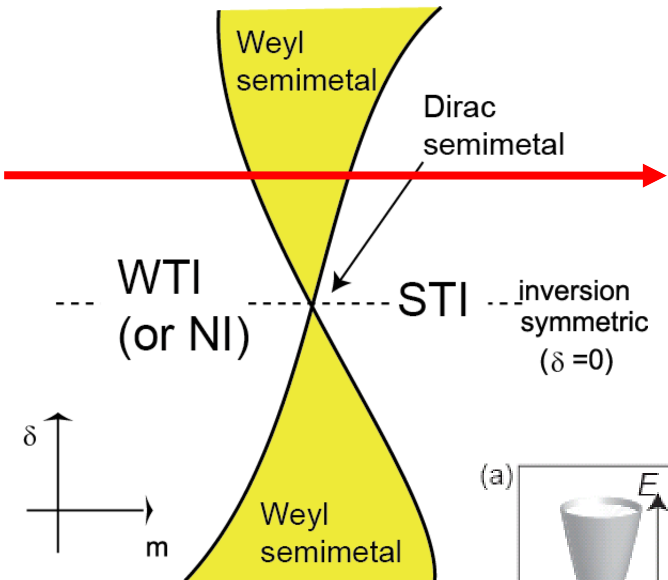

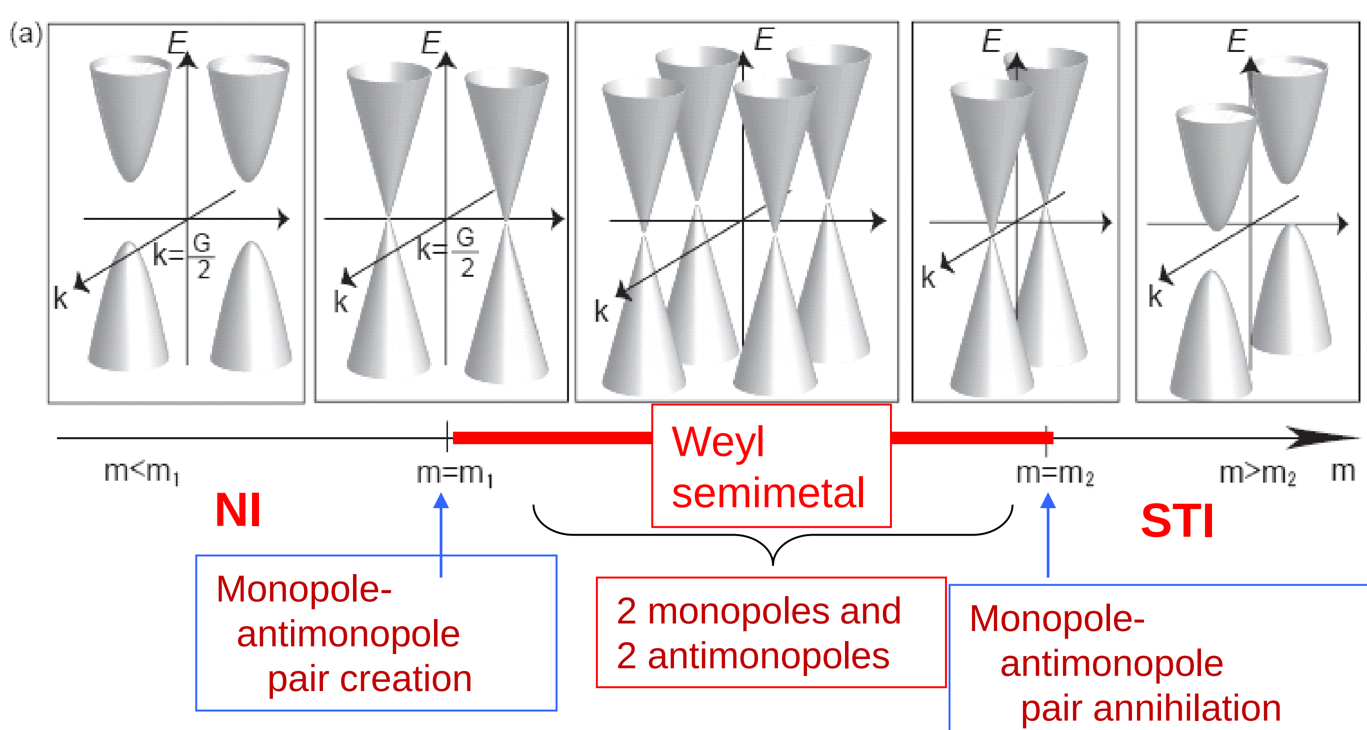

3D Weyl nodes = monopole or antimonopole for Berry curvature

$$\vec{B}_n(\vec{k}) = i\left\langle \frac{\partial u_{nk}}{\partial \vec{k}} \right| \times \left| \frac{\partial u_{nk}}{\partial \vec{k}} \right\rangle$$: Berry curvature

$$\rho_n(\vec{k}) = \frac{1}{2\pi}\nabla_{\vec{k}} \cdot \vec{B}_n(\vec{k})$$: monopole density

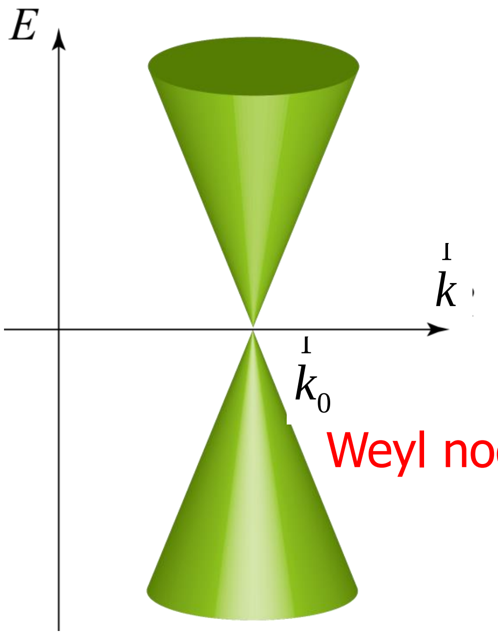

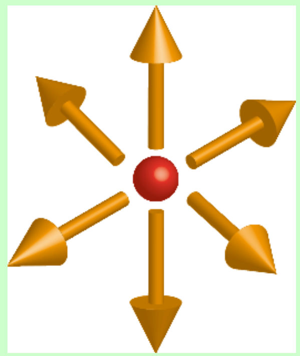

Monopole at $\vec{k} = \vec{k}_0$

$$\rho_l(\vec{k}) = \delta(\vec{k} - \vec{k}_0)$$

or

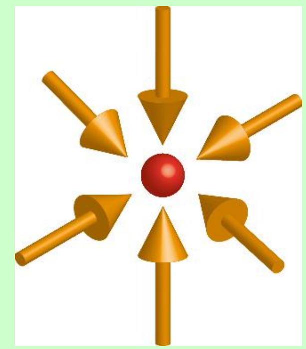

Antimonopole at $\vec{k} = \vec{k}_0$

$$\rho_l(\vec{k}) = -\delta(\vec{k} - \vec{k}_0)$$

- Weyl nodes are either monopole or antimonopole
- Quantized monopole charge

C. Herring, Phys. Rev. 52, 365 (1937).
G. E. Volovik, The Universe in a Helium Droplet (2007).
S. Murakami, New J. Phys. 9, 356 (2007).

Weyl semimetal

→ Bulk 3D Dirac cones without degeneracy

Either time-reversal or inversion symmetry must be broken

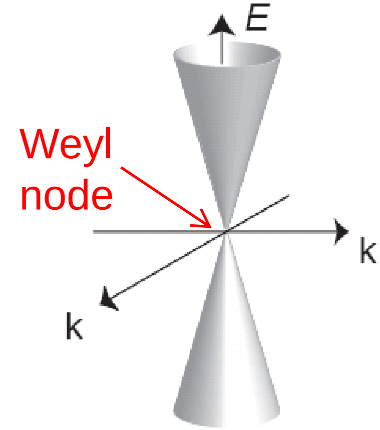

$\sim \mathbf{k} \cdot \boldsymbol{\sigma}$

SM, NJP ('07).

- Surface Fermi arc – connecting between Weyl nodes

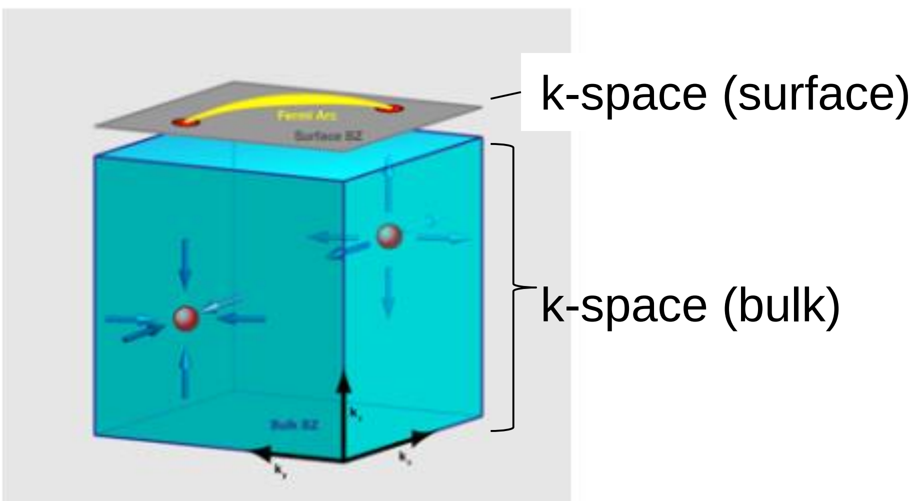

Balents, Physics **4**, 36 (2011)

•Dispersion of Femi arc

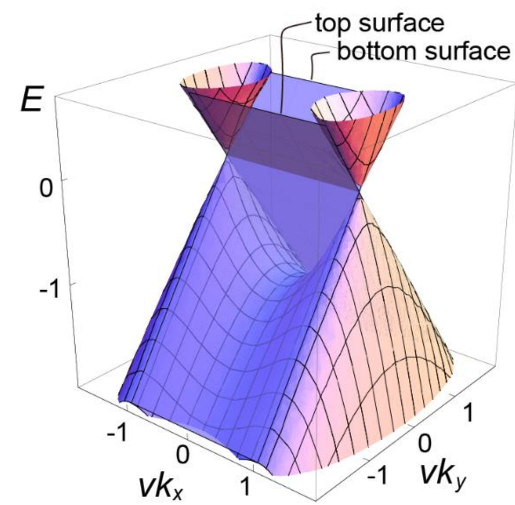

Okugawa, Murakami, Phys. Rev. B (2014)

Search for Weyl semimetals without inversion symmetry

Start from an insulator

→ suppose a gap closes by changing a parameter *m*

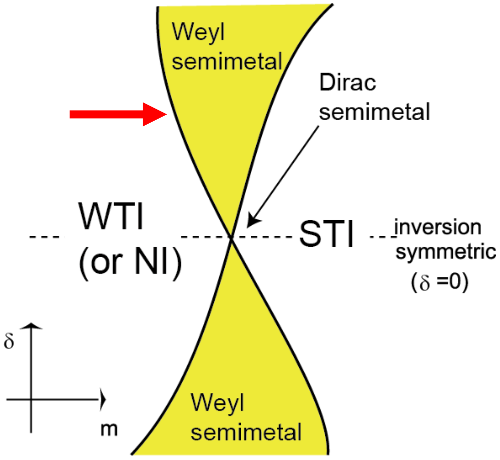

Classification by space groups & *k*-points.

230 space groups

138 space groups without inversion sym.

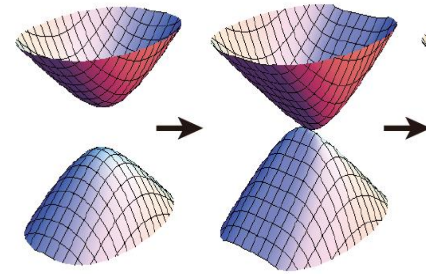

?

1	2	3	4	5	6	7	8	9	10	11	12	13	14	15	16	17	18	19	20
21	22	23	24	25	26	27	28	29	30	31	32	33	34	35	36	37	38	39	40
41	42	43	44	45	46	47	48	49	50	51	52	53	54	55	56	57	58	59	60
61	62	63	64	65	66	67	68	69	70	71	72	73	74	75	76	77	78	79	80
81	82	83	84	85	86	87	88	89	90	91	92	93	94	95	96	97	98	99	100
101	102	103	104	105	106	107	108	109	110	111	112	113	114	115	116	117	118	119	120
121	122	123	124	125	126	127	128	129	130	131	132	133	134	135	136	137	138	139	140
141	142	143	144	145	146	147	148	149	150	151	152	153	154	155	156	157	158	159	160
161	162	163	164	165	166	167	168	169	170	171	172	173	174	175	176	177	178	179	180
181	182	183	184	185	186	187	188	189	190	191	192	193	194	195	196	197	198	199	200
201	202	203	204	205	206	207	208	209	210	211	212	213	214	215	216	217	218	219	220
221	222	223	224	225	226	227	228	229	230										

No inversion sym.

156 $P3m1$ C_{3v}^1

($F1$; $K6$; $K7$; $M5$; $Z1$.)

Γ $\mathbf{G}_{12}^4$: $\{C_3^+ \mid 000\}$, $\{\sigma_{v1} \mid 000\}$: 3, 3; 4, 3; 6, 2: a.
M $\mathbf{G}_4^1 \otimes \mathbf{T}_2$: $\{\sigma_{v1} \mid 000\}$; $\mathbf{t}_2$: 2, 3; 4, 3: b.
A $\mathbf{G}_{12}^4 \otimes \mathbf{T}_2$: $\{C_3^+ \mid 000\}$, $\{\sigma_{v1} \mid 000\}$; $\mathbf{t}_3$: 3, 3; 4, 3; 6, 2: a.
L $\mathbf{G}_4^1 \otimes \mathbf{T}_2$: $\{\sigma_{v1} \mid 000\}$; $\mathbf{t}_2$ or $\mathbf{t}_3$: 2, 3; 4, 3: b.

high-symmetry points (TRIM)

K $\mathbf{G}_6^1 \otimes \mathbf{T}_3$: $\{C_3^+ \mid 000\}$; $\mathbf{t}_1$ or $\mathbf{t}_2$: 2, 2; 4, 2; 6, 2: a.
H $\mathbf{G}_6^1 \otimes \mathbf{T}_3 \otimes \mathbf{T}_2$: $\{C_3^+ \mid 000\}$; $\mathbf{t}_1$ or $\mathbf{t}_2$; $\mathbf{t}_3$: 2, 2; 4, 2; 6, 2: a.

high-symmetry points (non TRIM)

Δ^x $\mathbf{G}_{12}^4$: $(C_3^+, 0)$, $(\sigma_{v1}, 0)$: 3, x; 4, x; 6, x: a.
U^x $\mathbf{G}_4^1$: $(\sigma_{v1}, 0)$: 2, x; 4, x: b.
P^x $\mathbf{G}_6^1$: $(C_3^+, 0)$: 2, x; 4, x; 6, x: a.
T^x $\mathbf{G}_2^1$: $(\bar{E}, 0)$: 2, 2: a.
S^x $\mathbf{G}_2^1$: $(\bar{E}, 0)$: 2, 2: a.
T'^x $\mathbf{G}_2^1$: $(\bar{E}, 0)$: 2, 2: a.
S'^x $\mathbf{G}_2^1$: $(\bar{E}, 0)$: 2, 2: a.
Σ^x $\mathbf{G}_4^1$: $(\sigma_{v1}, 0)$: 2, x; 4, x: b.
R^x $\mathbf{G}_4^1$: $(\sigma_{v1}, 0)$: 2, x; 4, x: b.

high-symmetry lines

"The Mathematical Theory of Symmetry in Solids", Bradley, Cracknell

Each k point → k group

(Example): C_2 symmetry (i.e. k = invariant under C_2)

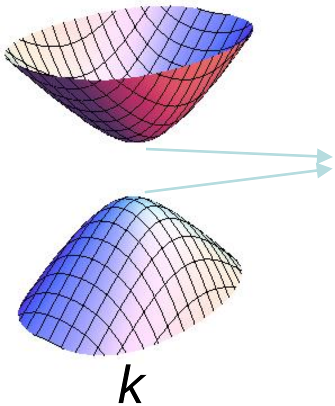

C_2 eigenvalue = +1 or -1

(i) <u>Same signs of C_2</u>

gap cannot close at k – level repulsion

(ii) <u>Different signs of C_2</u>

gap closing

→ Weyl semimetal

monopole-antimonopole pair creation

→ move along a symmetry line

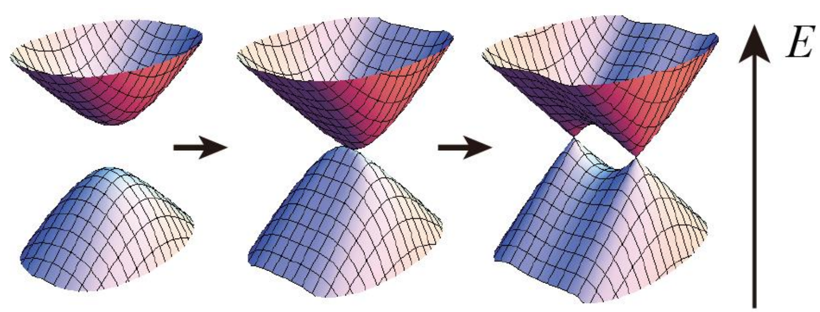

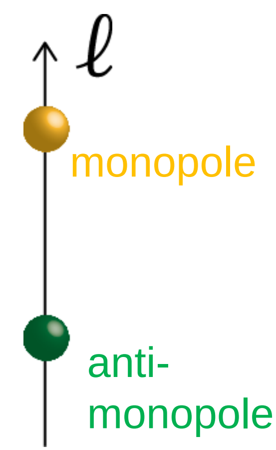

Systems without inversion symmetry
→ Classification of parametric gap-closing

(a) Metal （gap closes along a loop) – mirror symmetric

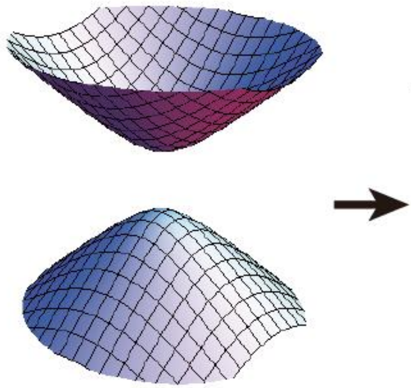

(b) Weyl semimetal

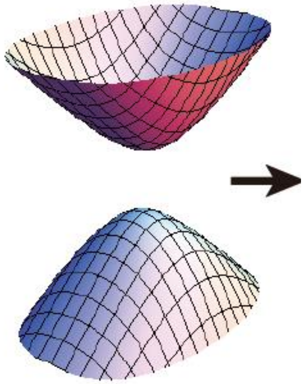

Only two possibilities. No insulator-to-insulator transition happens.

Topological Effects in Tellurium and Selenium

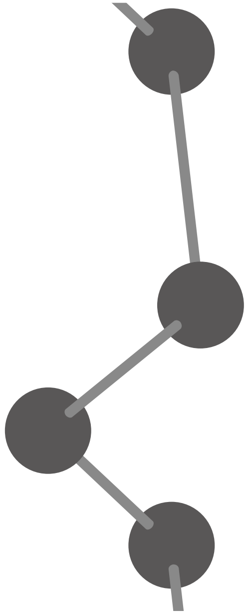

Hirayama, Okugawa, Ishibashi, Murakami, Miyake,
PRL 114, 206401 (2015)

Introduction

Group-VI elements : Te and Se

Trigonal:$P3_121$ or $P3_221$

(ex. :α-quartz)

the <u>strong SOI </u>with the <u>broken</u> space inversion symmetry

allows appearance of <u>Weyl nodes</u>

Band gap : Te 0.323, Se 2.0 (eV)

V. B. Anzin *et al.*, Phys. Stat. Sol. (a) **42**, 385 (1977).

S. Tutihasi *et al.*, Phys. Rev. **158**, 623 (1967).

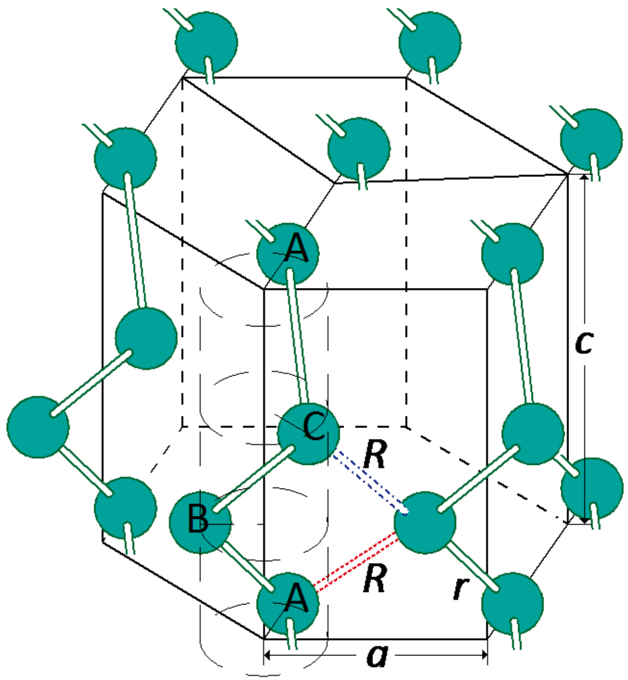

Structure of Te and Se

- <u>helical chains</u>
  either right-handed
  or left-handed

Electronic band structures of Te and Se

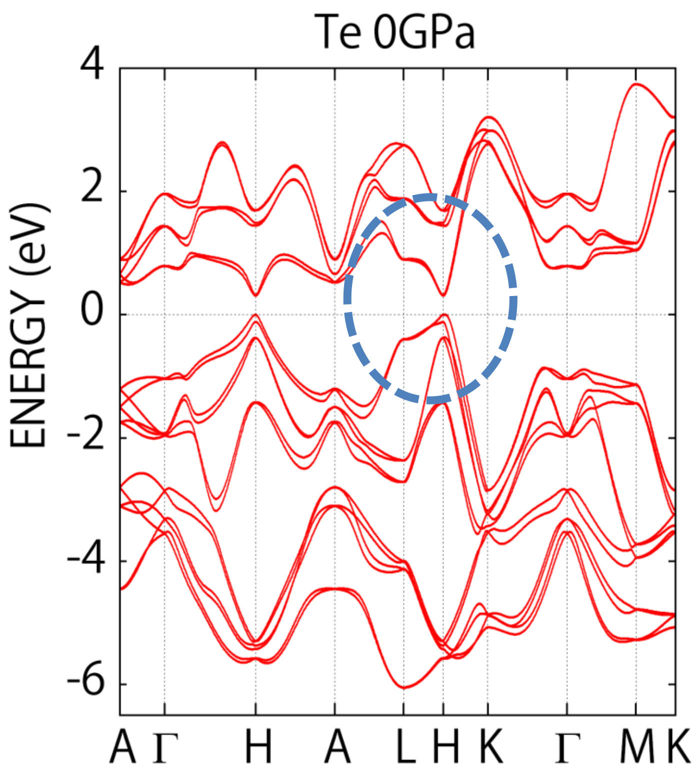

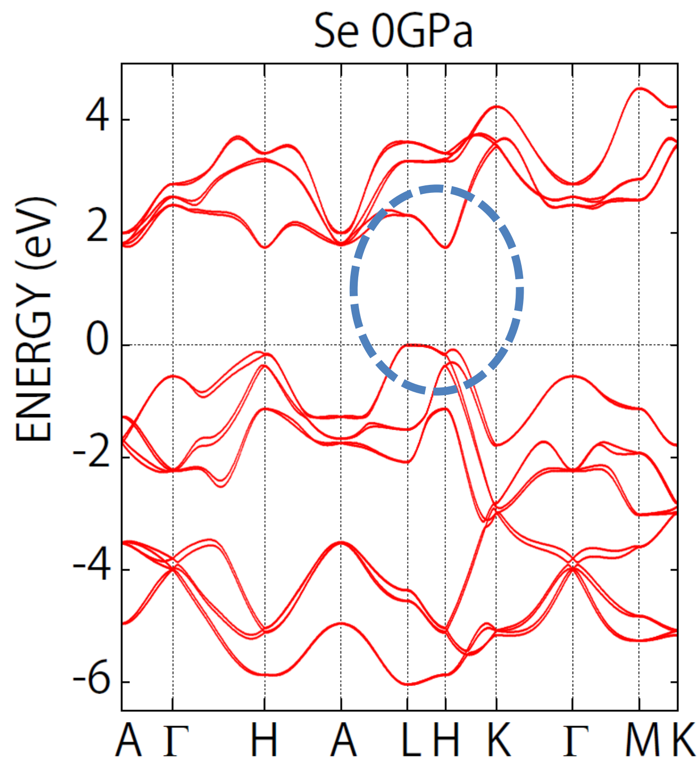

Band gap (*GW*+SO): Te 0.314, Se 1.74 (eV)

(exp.): Te 0.323, Se 2.0 (eV)

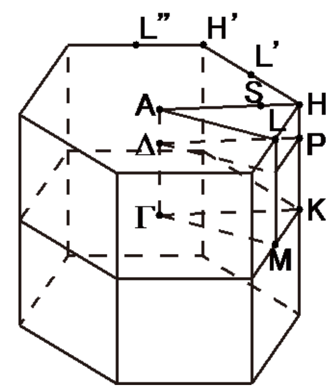

V. B. Anzin *et al.*, Phys. Stat. Sol. (a) **42**, 385 (1977).
S. Tutihasi *et al.*, Phys. Rev. **158**, 623 (1967).

Electronic band structure under pressure

Hirayama, et al.,
PRL 114, 206401 (2015)

Low → Increase pressure → High

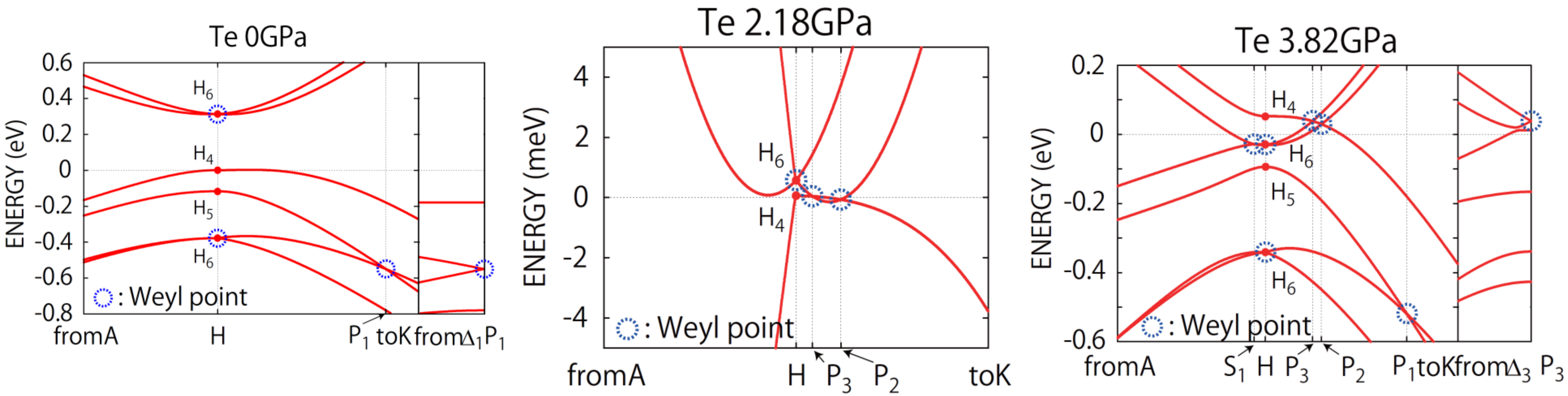

insulator

Weyl semimetal

metal

Te becomes the Weyl semimetal under pressure.

It is a first proposal of Weyl semimetals for real materials with broken inversion symmetry.

Motion of Weyl Nodes: topological nature

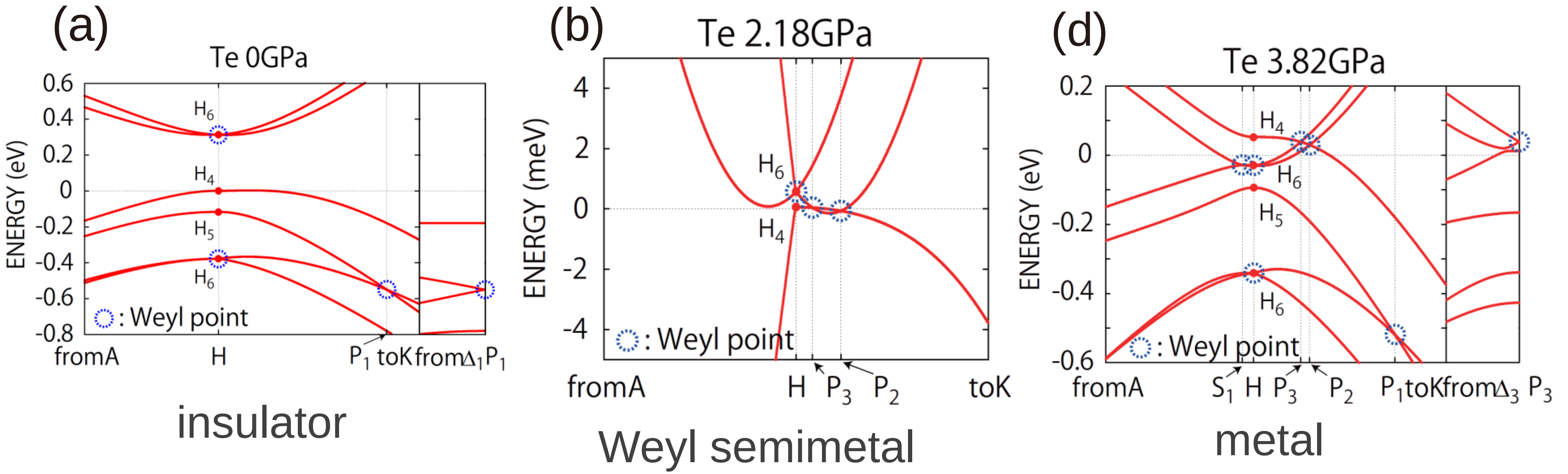

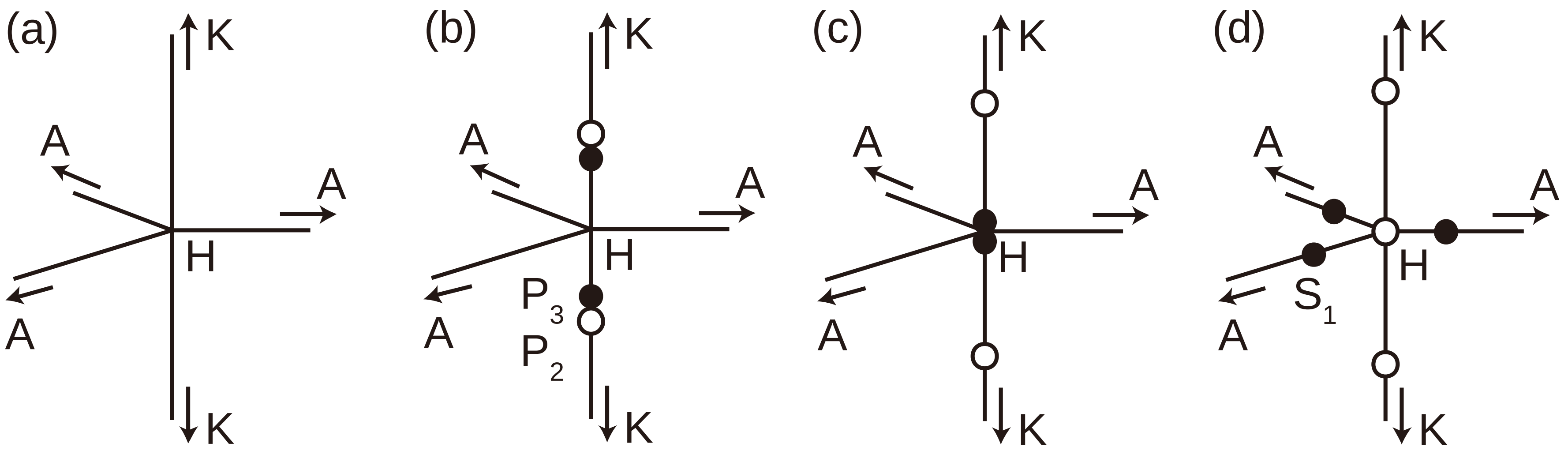

Low → Increase pressure → High

((a)→(b)→(c)→(d))

Fermi Surface and Spin Texture of Te

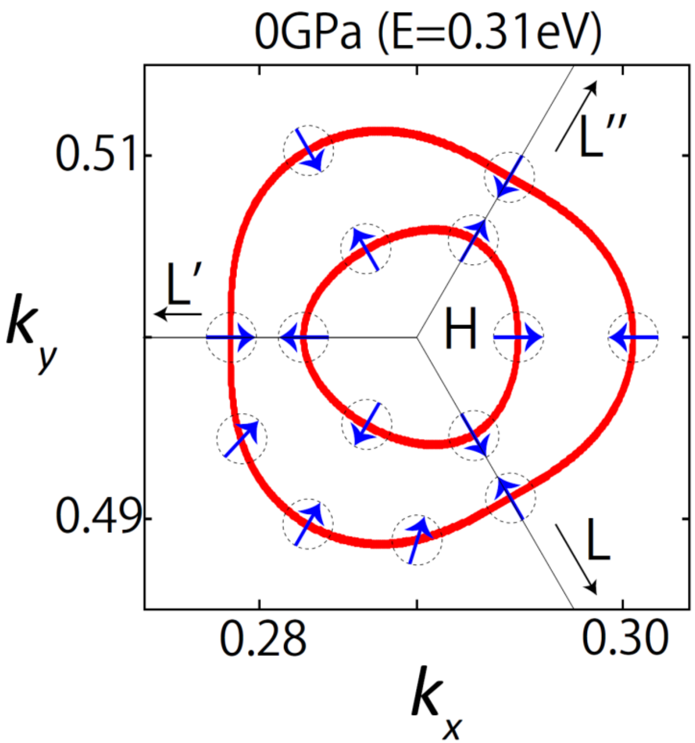

c.f. Rashba system

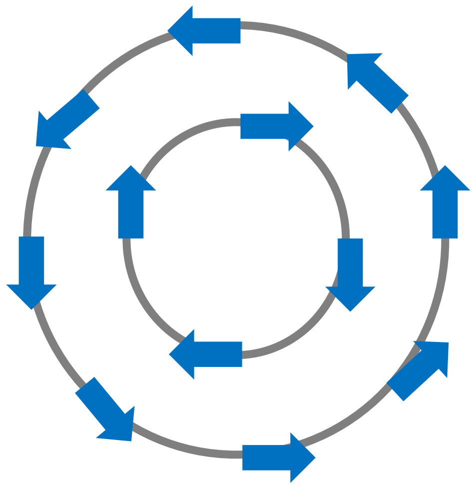

The Fermi surface around the H point has a hedgehog spin structure.

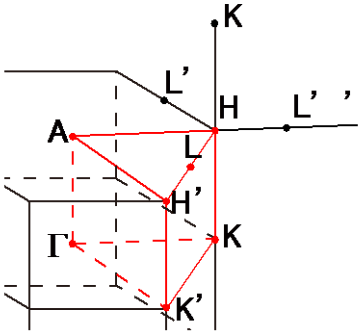

Hirayama, et al.,
PRL 114, 206401 (2015)

Chiral transport
in crystals with helical structure

current-induced orbital magnetization

Electric current flowing through a helical crystal generates a magnetization.

Magnetization

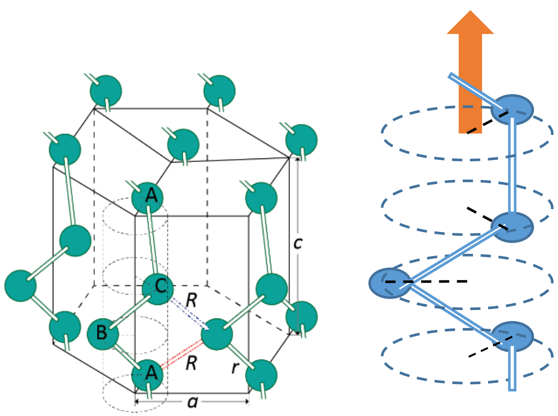

Electric current

Analogy to solenoid

Magnetic field

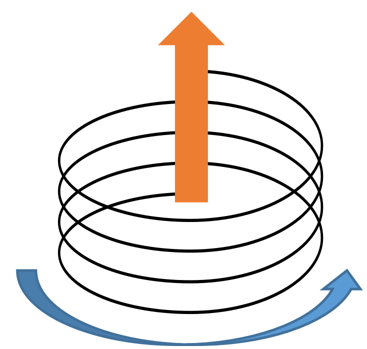

Electric current

Current-induced orbital magnetization

Model

An infinite stack of honeycomb lattice layers with a helical structure

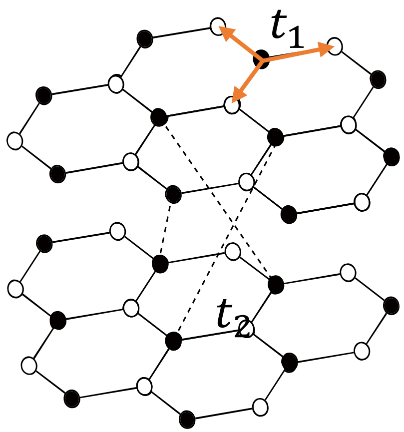

$$H = t_1 \sum_{\langle ij \rangle} c_i^\dagger c_j + t_2 \sum_i \xi_i c_i^\dagger c_j$$

t_1: nearest neighbor hopping

t_2: helical hopping between the same sublattice in the neighboring layers

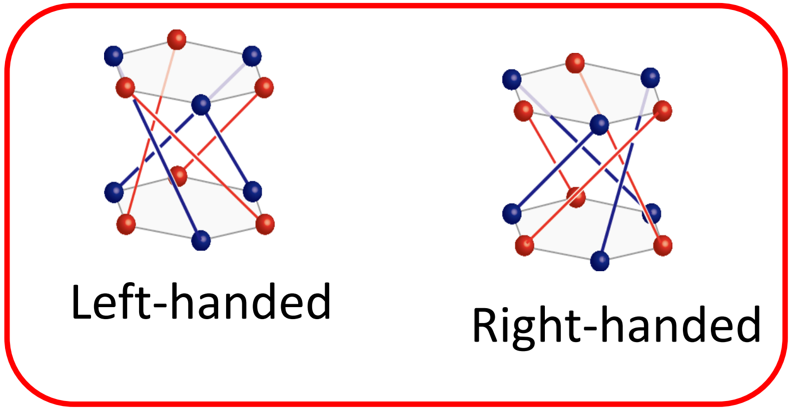

Formalism for current induced orbital magnetization

Orbital magnetization (Ceresoli et al, Xiao et al. (2006))

$$\boldsymbol{M}_{\mathrm{orb}} = \frac{e}{2\hbar}\mathrm{Im}\sum_{n}\int_{\mathrm{BZ}}\frac{d^3\boldsymbol{k}}{(2\pi)^3} f_{n\boldsymbol{k}}\langle\partial_{\boldsymbol{k}}u_{n\boldsymbol{k}}| \times (H_{\boldsymbol{k}} + \varepsilon_{n\boldsymbol{k}} - 2\varepsilon_F)|\partial_{\boldsymbol{k}}u_{n\boldsymbol{k}}\rangle$$

Apply electric field (// helical axis)

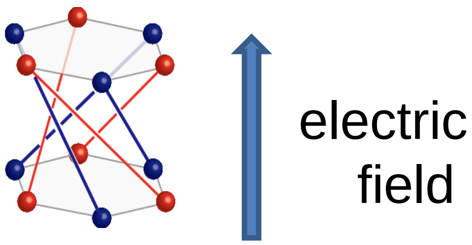

Boltzmann approximation

distribution function : $f_{n\boldsymbol{k}} = f^0_{n\boldsymbol{k}} + eE_z\tau v_{n,z}\left.\frac{df}{d\varepsilon}\right|_{\varepsilon=\varepsilon_{n\boldsymbol{k}}}$

For a metal, the orbital magnetization is induced by an electric current.

Result

parameters : $t_2 = t_1/3$

(a)Right-handed crystal

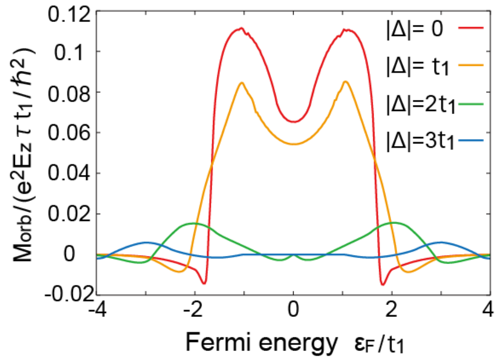

(b)Left-handed crystal

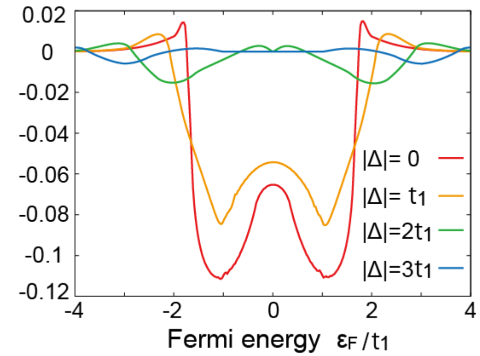

▪The directions of the magnetization is opposite for the right-handed and left-handed helix.

Quantum mechanical analog of solenoid!

▪The orbital magnetization is enhanced around the Dirac points.

Band structure for the right-handed helix

$\Delta = 1$

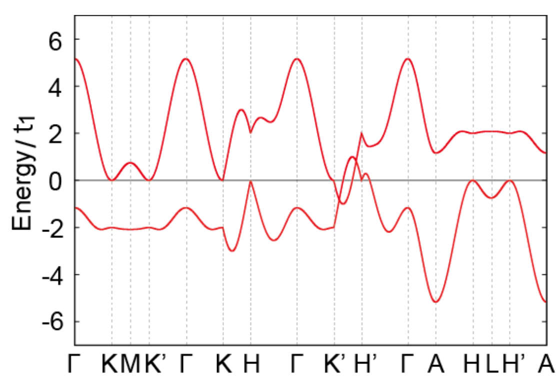

$\Delta = 3$

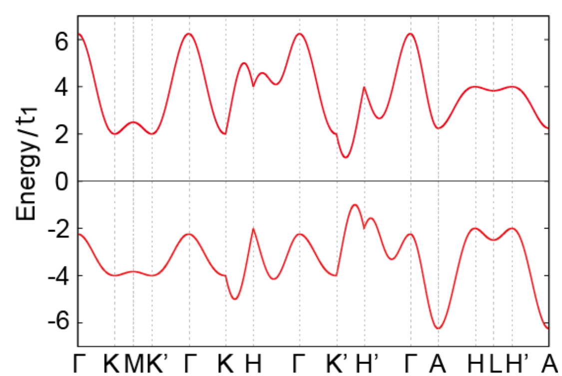

Current-induced spin magnetization

Spin-orbit coupling should be included

Model

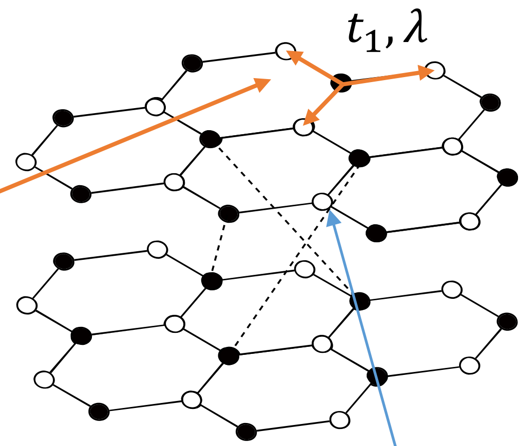

$$H = t_1 \sum_{\langle ij \rangle} c_i^\dagger c_j + \Delta \sum_i \xi_i c_i^\dagger c_j$$

$$+ \frac{i\sqrt{3}\lambda}{a} \sum_{\langle ij \rangle} c_i^\dagger c_j + \frac{i\lambda_{xy}}{a} \sum_{[ij]} c_i^\dagger (s^x d_{ij}^x + s^y d_{ij}^y) c_j + \frac{i\lambda_z}{c} \sum_{[ij]} c_i^\dagger s^z d_{ij}^z c_j$$

spin-orbit interaction

λ:spin-dependent nearest neighbor hopping

λ_{xy}, λ_z:spin-dependent helical hopping between the sublattice in the neighboring layers

Spin texture

Band structure: $t_1 = 1, \lambda = -0.06, \lambda_{xy} = 0.05, \lambda_z = 0.05$

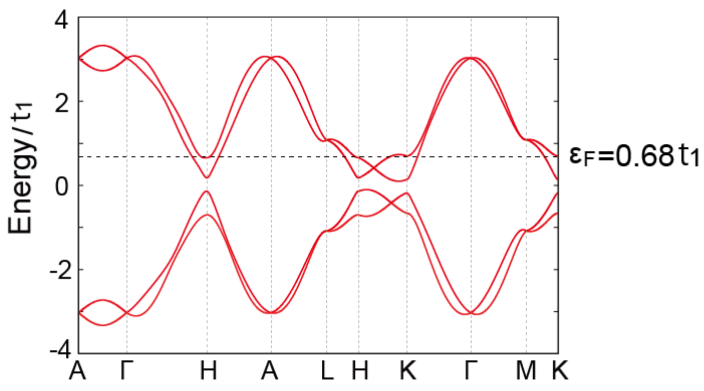

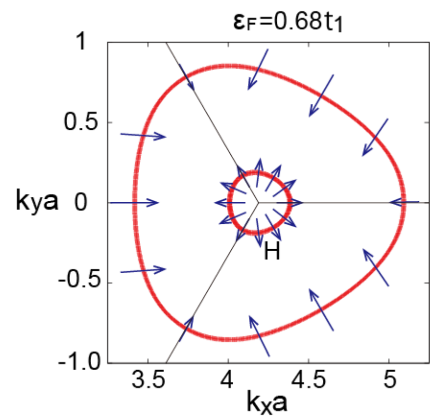

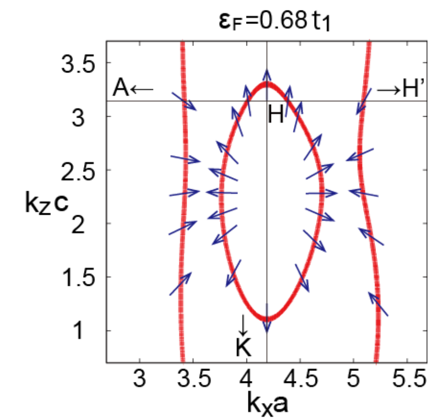

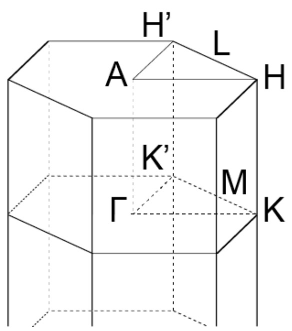

A radial spin texture around the H point (similar to Te)

Different from Rashba systems

Current-induced spin magnetization

We apply an electric field along the helical axis.

$$M_{\mathrm{spin},z} = -\frac{eE\tau\mu_B}{\hbar}\sum_n \int_{\mathrm{BZ}} \frac{d^3\boldsymbol{k}}{(2\pi)^3} \frac{df}{d\varepsilon}\bigg|_{\varepsilon=\varepsilon_{n\boldsymbol{k}}} \left\langle u_{n\boldsymbol{k}} \middle| \frac{\partial H_{\boldsymbol{k}}}{\partial k_z} \middle| u_{n\boldsymbol{k}} \right\rangle \langle u_{n\boldsymbol{k}} | s_z | u_{n\boldsymbol{k}} \rangle$$

z-component of spin magnetization

$$t_1 = 1, \lambda_{xy} = 0.05, \lambda_z = 0.05, \Delta = 0.4$$

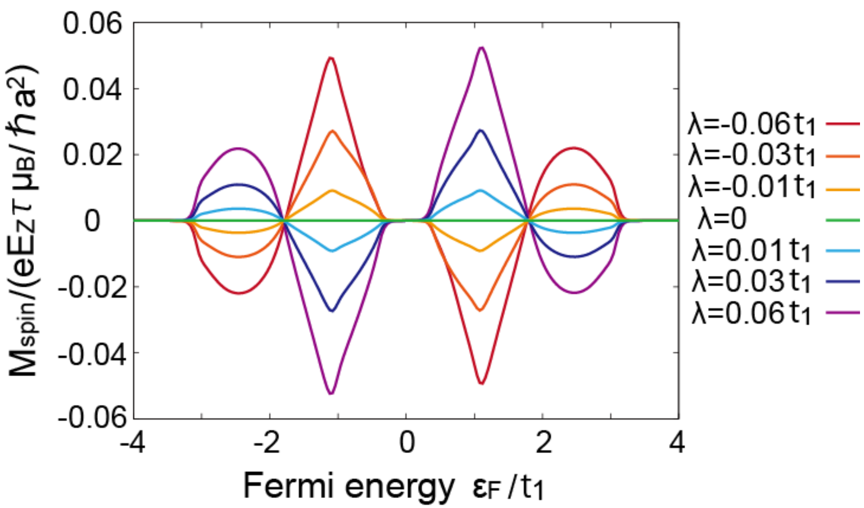

current-induced magnetization is parallel to a current (//helical axis)

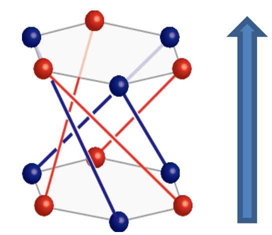

Current & magnetization

- Different from Rashba systems
- This comes from the radial spin texture

$E = 0$ $\qquad$ $E_z \neq 0, M_z \neq 0$

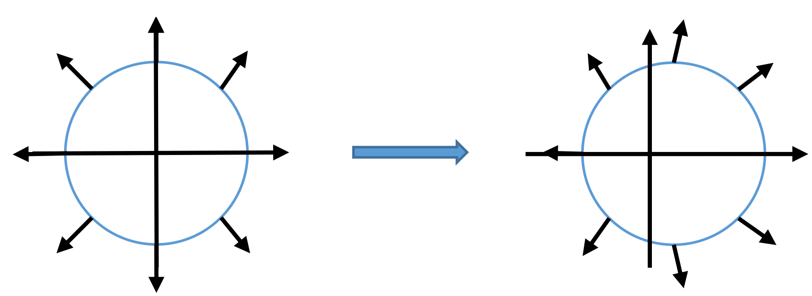

Chiral transport in CNTs

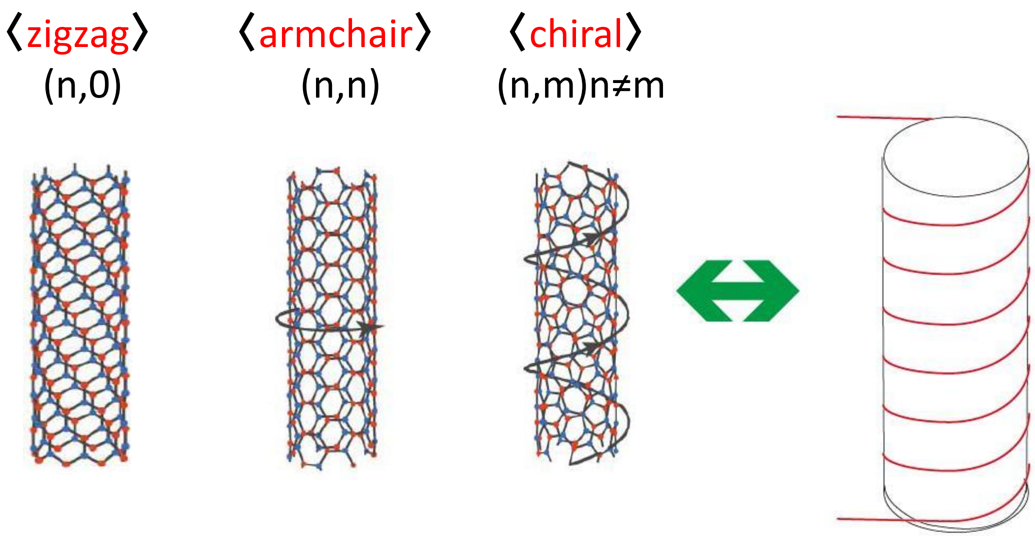

Chiral nanotube breaks inversion & mirror symmetries
→ chiral transport is allowed

〈previous works〉

Theoretical proposal in BC_2N — Y Miyamoto et al. PRB 50, 4976 (1994)

Magnetization for ballistic transport in CNT — N Tsuji et al. PRB 75, 153406 ('07)

Self-induction in CNT — B Wang et al. PRB 80, 235430 (2009)

Calculation of Chiral transport

〈Hamiltonian〉:

nearest-neighbor tight-binding model

〈conductivity〉:

Boltzmann transport,

constant relaxation time

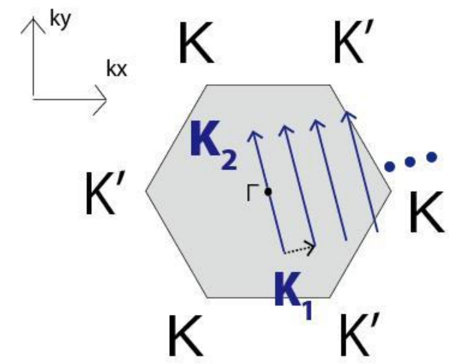

$$\sigma_{ij} = -e^2 \frac{1}{S} \sum_k v_i v_j \frac{\partial f \ (E_k)}{\partial E_k} \tau = \frac{e^2 \tau}{\hbar^2 S} \sum_{k_i k_j, E_f \geq E_k} \frac{\partial^2 E_k}{\partial k_i \partial k_j}$$

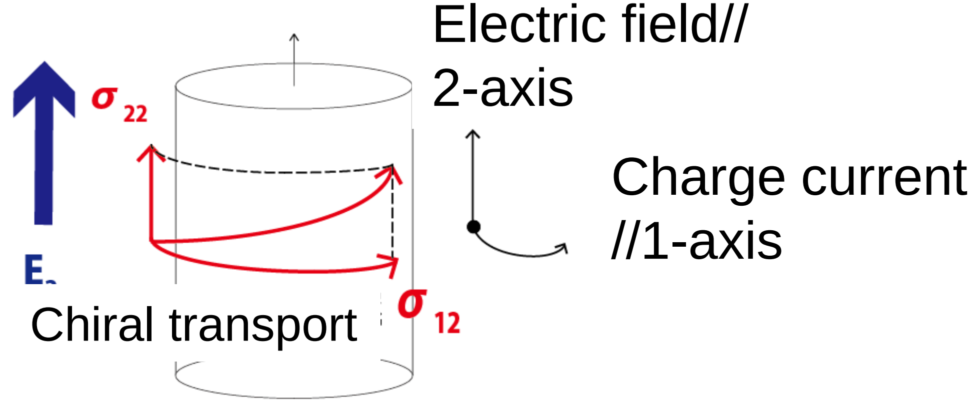

Chiral conductivity for nanotubes with various chiralities

(15,m) CNT

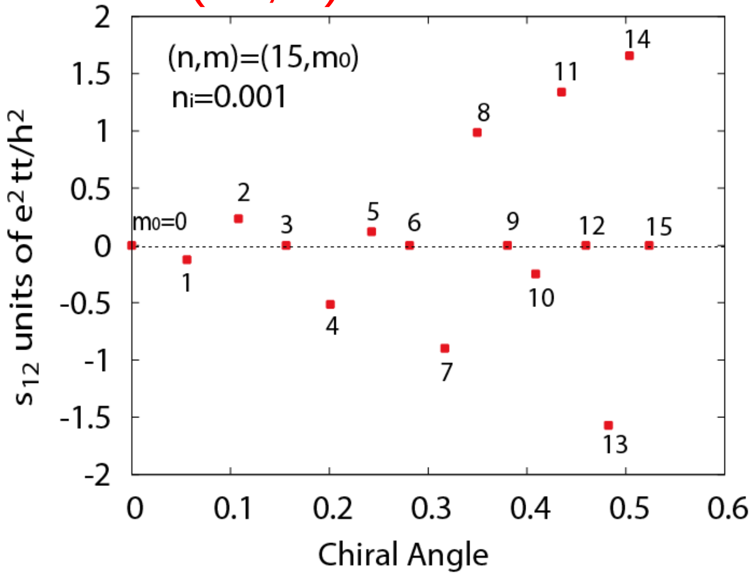

For fixed (small) carrier concentration…

- n-m=3N : σ_{12}=0
- n-m=3N+2: σ_{12}>0
- n-m=3N+1: σ_{12}<0

It can be understood from the warped Fermi surface

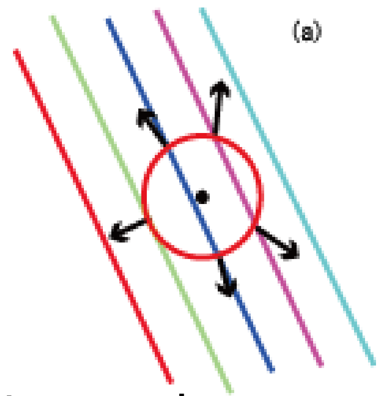

No warping: σ_{12}=0

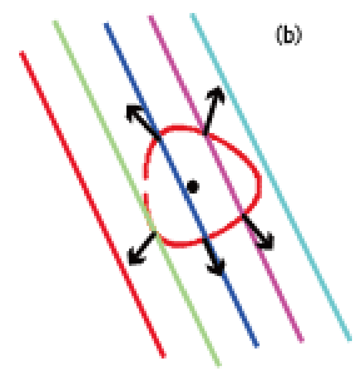

warping: σ_{12}: + or – depending on (n-m)

Chiral conductivity for (8,6) nanotube

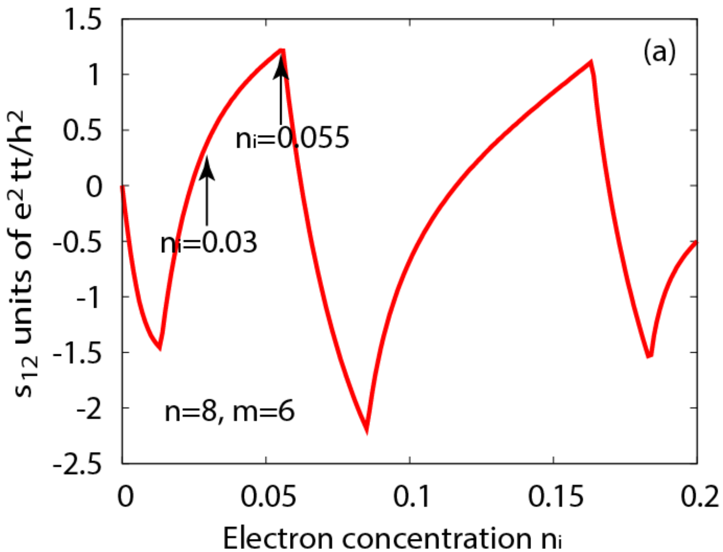

Kinks as a function of carrier concentration

→ Due to subband structures

Decompose into subband contributions:

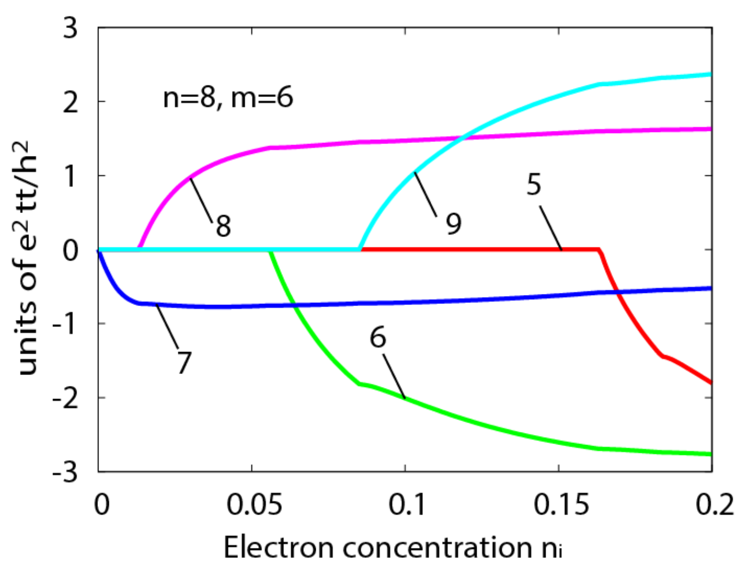

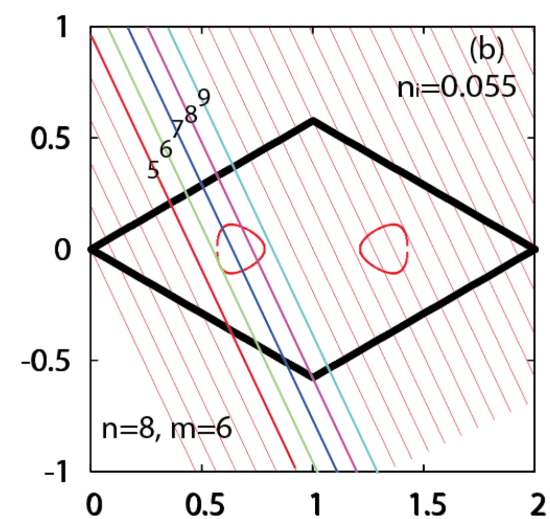

Conclusions

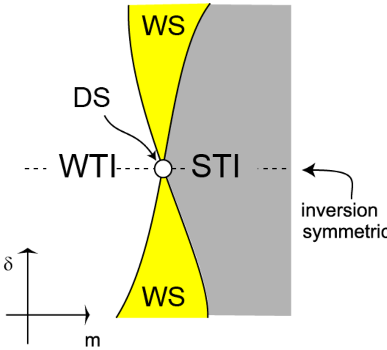

- Weyl semimetals (in inversion asymmetric systems)
  - In topological insulator (TI) – normal insulator (NI) phase transition, Weyl semimetals naturally appear
  - Combine with space group symmetry
    → powerful way for searching topological phases
    e.g. Tellurium: Weyl semimetal at high pressure
- Chiral transport in crystals with helical lattice structure
  - analogy with solenoid
  - Current induced orbital & spin magnetization
  - Example:
    - 3D chiral crystals: Tellurium etc.
    - chiral CNT